

## Chapter 3

# Atomic Hydrogen

‘The two most common things in the Universe  
are Hydrogen and Stupidity.’

– Harlan Ellison (1934)

### 3.1 Overview

Spectra of atomic hydrogen, H, are of paramount astronomical importance. This is because approximately 90% of atomic matter by number is hydrogen. This occurs in a variety of forms:  $H^+$  or protons, H atoms,  $H_2$  molecules and indeed the molecular ions  $H_2^+$  and  $H_3^+$ . The spectral lines of hydrogen are prominent in a great variety of astronomical objects and are much studied. All aspects of hydrogen spectroscopy therefore need to be considered in detail.

The spectrum of atomic hydrogen also plays an important role in the theory of quantum mechanics. Hydrogen is the simplest atom, comprising a single electron and a proton. It is the only atom for which exact quantum mechanical solutions can be found for its energy levels and wavefunctions. These solutions will be used extensively here but will not be derived. Such derivations are a standard part of most introductory courses in quantum physics [see Rae (2002) in further reading].

### 3.2 The Schrödinger Equation of Hydrogen-Like Atoms

Any atom comprising a single electron orbiting a nucleus of charge  $Z$  can be described as hydrogen-like. The Hamiltonian operator for this system

can be written

$$\hat{H} = \frac{-\hbar^2}{2\mu} \nabla^2 - \frac{Ze^2}{4\pi\epsilon_0 r}, \quad (3.1)$$

where  $\underline{r}$  is a vector, of length  $r$ , linking the electron to the nucleus. This Hamiltonian comprises two terms. The first term, given by the Laplacian operator, is the kinetic energy operator for the electron. The second term is the potential energy term, in this case the Coulomb attraction between the electron, charge  $-e$ , and the nucleus, charge  $+Ze$ .

The Hamiltonian (3.1) contains a number of constants. It is often given in terms of atomic units, which scale the dimensions of the problem to the atomic scale. In atomic units (see Sec. 3.4 for details), the charge on an electron  $e$ , the mass of an electron  $m_e$ ,  $\hbar = \frac{h}{2\pi}$  and  $4\pi\epsilon_0$  all equal one. This simplifies the Hamiltonian to:

$$\hat{H} = -\frac{1}{2\mu} \nabla^2 - \frac{Z}{r}. \quad (3.2)$$

In general the Schrödinger equation for a system of energy  $E$  and with wavefunction  $\psi$  is written

$$\hat{H}\psi = E\psi. \quad (3.3)$$

For the particular case of the hydrogen-like atom in atomic units, the explicit form of the Schrödinger equation is therefore

$$\left[ -\frac{1}{2\mu} \nabla^2 - \frac{Z}{r} - E \right] \psi(\underline{r}) = 0. \quad (3.4)$$

### 3.3 Reduced Mass

The hydrogen atom is actually a two-particle problem, concerning the motion of an electron of mass  $m_e$  and a nucleus of mass  $M$ . To solve for the internal motion of this system it is necessary to rewrite the equations-of-motion of the system into one equation representing the overall translation of the whole system, with mass  $M + m_e$ , in space, and a second equation representing the internal motions. The Schrödinger equation (3.4) is the quantum mechanical equation representing this internal motion of the hydrogen atom once the equations governing the translational motion of the whole system through space have been separated. In this Schrödinger equation, the effective mass of the reduced system is denoted  $\mu$  and is known as the *reduced mass*.

For a system with two particles of mass  $m_1$  and  $m_2$ ,

$$\mu = \frac{m_1 m_2}{m_1 + m_2}. \quad (3.5)$$

Clearly, if  $m = m_1 = m_2$ , then  $\mu = \frac{m}{2}$ .

For the case of the hydrogen-like atom,

$$\mu = \frac{m_e M}{M + m_e}. \quad (3.6)$$

In the limit of an infinite nuclear mass, i.e.  $M = \infty$ ,  $\mu = m_e$ . In practice,  $M$  is very much bigger than  $m_e$ . For example, for H itself,  $M$  is about  $1836 m_e$ . Under these circumstances the reduced mass is very close to  $m_e$ . However, as discussed in Secs. 3.7 and 3.11, the small shift implied by a correct treatment of the reduced mass is important for astronomical observations as it means that hydrogen and deuterium give distinct spectra that can be distinguished at moderate resolution.

### 3.4 Atomic Units

Atomic units provide a complete integrated unit system in the manner of SI units but with quantities scaled to the dimensions of the atom. In atomic units:

Unit of mass is the electron mass,  $m_e = 1.6605402 \times 10^{-27}$  kg,

Unit of electric charge is the electron charge,  $e = 1.602188 \times 10^{-19}$  C,

Unit of length, the Bohr radius  $a_0 = \frac{4\pi\epsilon_0\hbar^2}{me^2} = 5.29177249 \times 10^{-11}$  m,

Planck's constant divided by  $2\pi$ ,  $\hbar = 1$  a.u. =  $1.05457 \times 10^{-34}$  J·s,

Similarly  $4\pi\epsilon_0 = 1$ .

In this unit system, the atomic unit of energy is known as the Hartree and is denoted  $E_h$ .  $1E_h = 2R_\infty = 27.2113661$  eV =  $4.3597482 \times 10^{-18}$  J, where  $R_\infty$  is the Rydberg constant (see Sec. 3.7). The atomic unit of time is  $2.41884 \times 10^{-17}$  s and the speed of light  $c$  is 137.03599 a.u.

Atomic units are often denoted a.u. and must be carefully distinguished from the somewhat larger Astronomical Unit, AU, or indeed the less well-defined 'arbitrary units'.

### 3.5 Wavefunctions for Hydrogen

The Schrödinger equation (3.4) can be solved analytically by working in spherical polar coordinates, i.e.  $\underline{r} = (r, \theta, \phi)$ . In these coordinates the wavefunction is separable into radial and angular solutions

$$\psi(r, \theta, \phi) = R_{nl}(r)Y_{lm}(\theta, \phi). \quad (3.7)$$

The radial solutions,  $R_{nl}$ , can be expressed analytically in terms of Laguerre polynomials [see Rae (2002) in further reading]. Figure 3.1 shows both the wavefunctions and the probability distribution of the lowest few

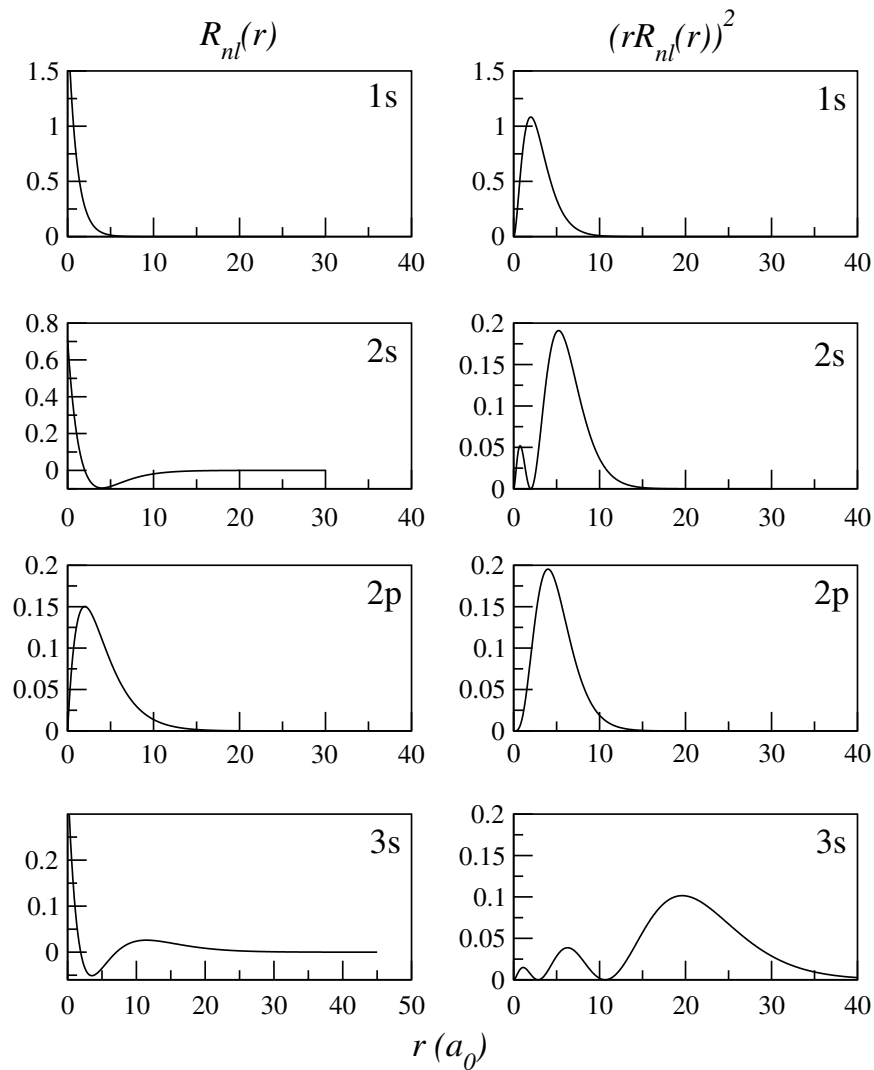


Fig. 3.1 Wavefunctions (*left*) and probability distribution (*right*) for the radial coordinate of the hydrogen atom. (T.S. Monteiro, private communication.)

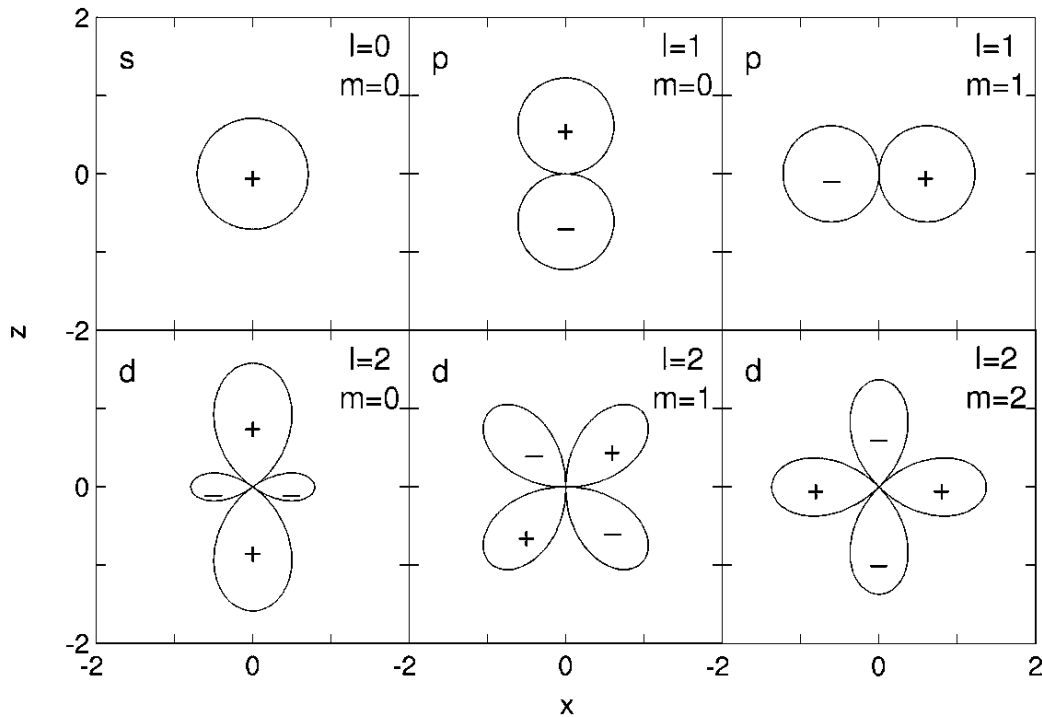


Fig. 3.2 Wavefunctions for the angular motions of the hydrogen atom which are given in terms of spherical harmonics,  $Y_{l,m}(\theta, \phi)$ . Plots are for the  $x-z$  plane except for the  $l = 2, m = 2$  plot for which the  $x-y$  plane is shown. The plots give the absolute value of the spherical harmonic as a distance from the origin for each angle; the signs indicate the sign of the wavefunction in each region. (S.A. Morgan, private communication.)

radial solutions. An important feature of these wavefunctions is the nodes which are the points where the wavefunctions pass through zero.

The angular solutions for the hydrogen atoms,  $Y_{l,m}$ , are called *spherical harmonics*. These functions are complex for  $m \neq 0$ . Figure 3.2 depicts the first few of these spherical harmonics. Readers familiar with chemistry will recognise these shapes as the s, p and d orbitals used to represent atomic structure and chemical bonds.

### 3.6 Energy Levels and Quantum Numbers

For bound states, the solutions of the Schrödinger equation (3.4) occur with discrete energies given by the formula

$$E_n = -\frac{\mu Z^2 e^4}{8h^2 \epsilon_0^2} \frac{1}{n^2} = -R \frac{Z^2}{n^2}, \quad (3.8)$$

where the zero of energy is taken to be a completely separated electron and nucleus with zero kinetic energy. The constant  $R$  in Eq. (3.8) is the *Rydberg constant* discussed in the next section.

Each bound state of the H atom is usually characterised by a set of four quantum numbers  $(n, l, m, s_z)$ . Each of these is defined below, along with a fifth quantum number  $s$ .

$n$  is the principal quantum number. It takes the values  $n = 1, 2, 3, \dots, \infty$ .  $n$  determines the energy of the atom according to Eq. (3.8).

$l$  is the electron orbital angular momentum quantum number. The actual angular momentum is given by  $\hbar[l(l+1)]^{\frac{1}{2}}$ .  $l$  can take the values  $0, 1, 2, \dots, n-1$ . By convention, the values of  $l$  are usually designated by letters (see Table 3.1).

$m$  is the magnetic quantum number, so called because it determines the behaviour of the energy levels in the presence of a magnetic field.  $m\hbar$  is the projection of the electron orbital angular momentum, given by  $l$ , along the  $z$ -axis of the system. It can take  $(2l+1)$  values  $-l, -l+1, \dots, 0, \dots, l-1, l$ .

$s$  is the electron spin quantum number. The electron spin angular momentum is given by  $\hbar[s(s+1)]^{\frac{1}{2}}$  which, for a one-electron system, equals  $\frac{\sqrt{3}}{2}\hbar$ , since an electron always has spin one-half.

$s_z$  gives the projection of the electron spin angular momentum, given by  $s$ , along the  $z$ -axis of the system. This projection is actually  $\hbar s_z$ . In general,  $s_z$  can take  $(2s+1)$  values given by  $-s, -s+1, \dots, s-1, s$ . For a one-electron system, this means  $s_z$  can take one of two values:  $-\frac{1}{2}$  or  $+\frac{1}{2}$ .

The simplest notations for the various states of H is to denote each state by its  $nl$  quantum numbers. Thus the ground state is denoted 1s; the first excited states are 2s and 2p; the  $n=3$  states are 3s, 3p and 3d. (See Fig. 3.3.) These notations leave the  $m$  and  $s_z$  quantum numbers unspecified since these quantum numbers are really only significant for H in the presence of an external field. This means that each  $nl$  configuration is  $2(2l+1)$ -fold degenerate. Such configurations are used to build up basic atomic struc-

Table 3.1 Letter designations for orbital angular momentum quantum number  $l$ .

0	1	2	3	4	5	6	7	8	...
s	p	d	f	g	h	i	k	l	...

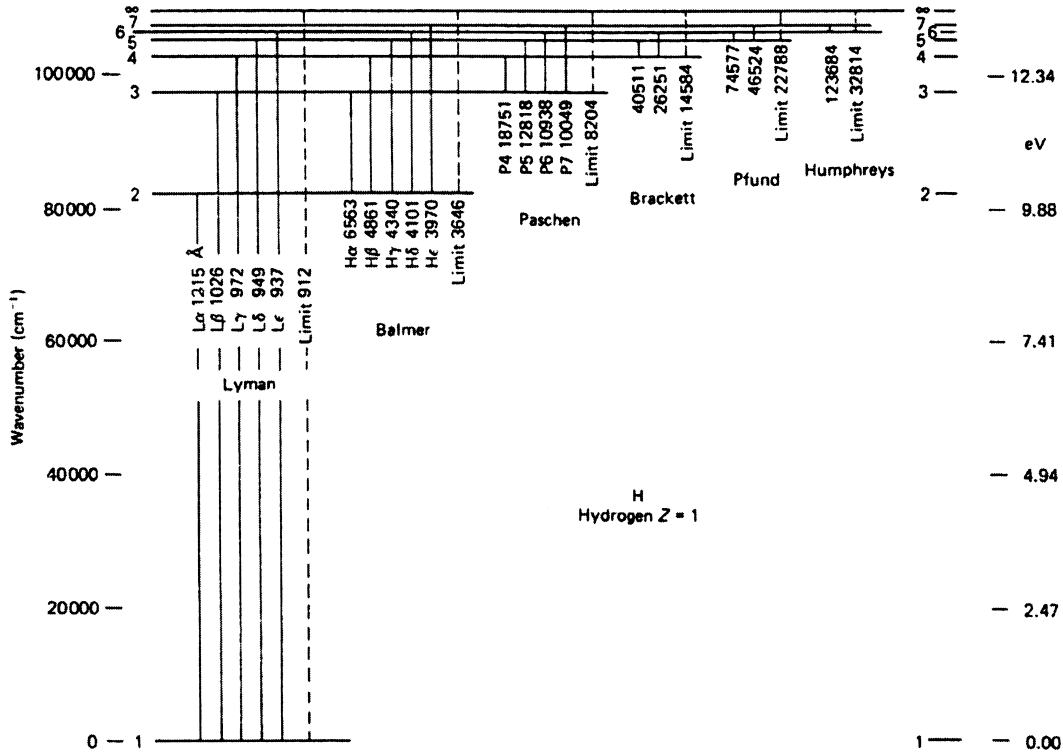


Fig. 3.3 Schematic energy levels of the hydrogen atom with various spectral series identified; vertical numbers are wavelengths in Å. [Adapted from P.W. Merrill, *Lines of the Chemical Elements in Astronomical Spectra* (Carnegie Institute of Washington Publications, 1956).]

ture (see Sec. 4.4). More complete and complicated spectroscopic notations used to denote states of H and other atoms are discussed in Sec. 4.8.

### 3.7 H-Atom Discrete Spectra

The spectrum of the hydrogen atom comes from electrons jumping between different levels in the atom. Given that the energy levels depend only on the quantum number  $n$ , this means that the electronic spectrum of the H atom comes from changes in  $n$ . The wavelengths,  $\lambda$ , for these transitions are given by the Rydberg formula:

$$\frac{1}{\lambda} = \frac{1}{hc}(E_{n_1} - E_{n_2}) = R_H \left( \frac{1}{n_1^2} - \frac{1}{n_2^2} \right), \quad n_1 < n_2. \quad (3.9)$$

This formula was constructed by the Swedish physicist Johannes Rydberg (1854–1919) to model the experimental observations of Balmer and others.

Of course, the formula agrees perfectly with the energy differences that one obtains using the quantum mechanical expression for the energy levels given in Eq. (3.8). In this expression,  $R$  is the Rydberg constant. This constant takes slightly different values for different H-like atoms since it incorporates the reduced mass  $\mu$  (see Sec. 3.3). For hydrogen itself,  $R_{\text{H}}$  is particularly well-determined experimentally; it takes the value  $109677.581 \text{ cm}^{-1}$ .

The Rydberg constant for a system of infinite nuclear mass is denoted by  $R_{\infty}$  and is related to  $R_{\text{H}}$  by

$$R_{\text{H}} = \frac{\mu}{m_e} R_{\infty} = \left( \frac{M_{\text{H}}}{M_{\text{H}} + m_e} \right) R_{\infty}, \quad (3.10)$$

where  $R_{\infty} = 109737.31 \text{ cm}^{-1}$ . Rydberg constants for other species such as deuterium, can be derived using the formula above with the appropriate reduced mass.

The spectrum of H is divided into a number of series linking different upper levels  $n_2$  with a single lower level  $n_1$  value. Each series is denoted according to its  $n_1$  value and is named after its discoverer. Table 3.2 summarises the six main H-atom series.

The range of each H-atom series is given by the lowest frequency transition, between the levels  $n_1$  and  $n_2 = n_1 + 1$ , and the *series limit*, which is the transition between  $n_1$  and  $n_2 = \infty$ . As discussed in Sec. 3.8.1, the series limit is not always observable. Table 3.2 gives the spectral region in which each series is observed. As the Balmer series lies in the visible region, it is particularly easy to observe from Earth. As a result, Balmer lines have been particularly important in the study of H-atom spectra.

Within a given series, individual transitions are labelled by Greek letters. These letters denote the change in  $n$  or  $\Delta n$ . In this notation:

$$\begin{aligned} \Delta n = 1 & \text{ is } \alpha, \\ \Delta n = 2 & \text{ is } \beta, \\ \Delta n = 3 & \text{ is } \gamma, \\ \Delta n = 4 & \text{ is } \delta, \\ \Delta n = 5 & \text{ is } \epsilon. \end{aligned}$$

Thus Ly $\alpha$  is the transition between  $n_1 = 1$  and  $n_2 = 2$ , and H $\gamma$  is that between  $n_1 = 2$  and  $n_2 = 5$ . Greek letters are usually only used for the most important transitions with low  $\Delta n$ . Transitions with high  $\Delta n$  are commonly labelled by the number  $n_2$ . Thus, H15 is the Balmer series transition between  $n_1 = 2$  and  $n_2 = 15$ .

Table 3.2 Spectral series of the H atom. Each series comprises the transitions  $n_2 - n_1$ , where  $n_1 < n_2 < \infty$ .

$n_1$	Name	Symbol	Spectral region	Range/cm <sup>-1</sup>	
				$n_2 = n_1 + 1$	$n_2 = \infty$
1	Lyman	Ly	ultraviolet	82257	– 109677
2	Balmer	H	visible	15237	– 27427
3	Paschen	P	infrared	5532	– 12186
4	Brackett	Br	infrared	2468	– 6855
5	Pfund	Pf	infrared	1340	– 4387
6	Humphreys	Hu	infrared	808	– 3047

The wavelength of each individual transition can be predicted using the Rydberg formula. For example Ly $\alpha$  lies at

$$\frac{1}{\lambda} = R_{\text{H}} \left( 1 - \frac{1}{4} \right) = \frac{3}{4} R_{\text{H}} = 82258.2 \text{ cm}^{-1}, \quad (3.11)$$

meaning that

$$\lambda = 1.21568 \times 10^{-5} \text{ cm} = 1215.68 \text{ \AA} = 121.168 \text{ nm}.$$

All hydrogen series transitions between bound states are described as bound-bound transitions. Figures 3.4, 3.5, 3.6 and 3.7 give sample H-atom spectra recorded in very different astronomical environments. Figure 3.4 shows an optical spectrum of the B-type star  $\Theta^1$  B Ori. Absorption by the Balmer series up to H14 ( $n_2 = 14$ ) is clearly visible. Figure 3.5 shows Lyman series absorption in a shell of gas expanding about a hot, Wolf-Rayet star. Figure 3.6 shows higher members of the Paschen series recorded in absorption in a spectrum from a soft X-ray transient binary star. Figure 3.7 shows infrared emissions due to Pfund and Brackett lines recorded in the gas ejected from supernova 1987a.

The reduced mass factor means that deuterium spectral lines are shifted with respect to H-atom spectra. In principle, one can detect D and H together (see Fig. 3.8). However, the cosmic abundance of deuterium is about  $2 \times 10^{-5}$  that of hydrogen. This makes it difficult to measure abundance ratios directly using neighbouring transitions as the H transitions are likely to be optically thick if those of D can be observed. Figure 3.9 shows high-resolution simultaneous observations of heavily red-shifted H and D Ly $\alpha$  lines. These data need to be interpreted very carefully since H absorptions with a different Doppler shift to the main peak, such as the peak on the left of the figure, can be confused with absorptions by

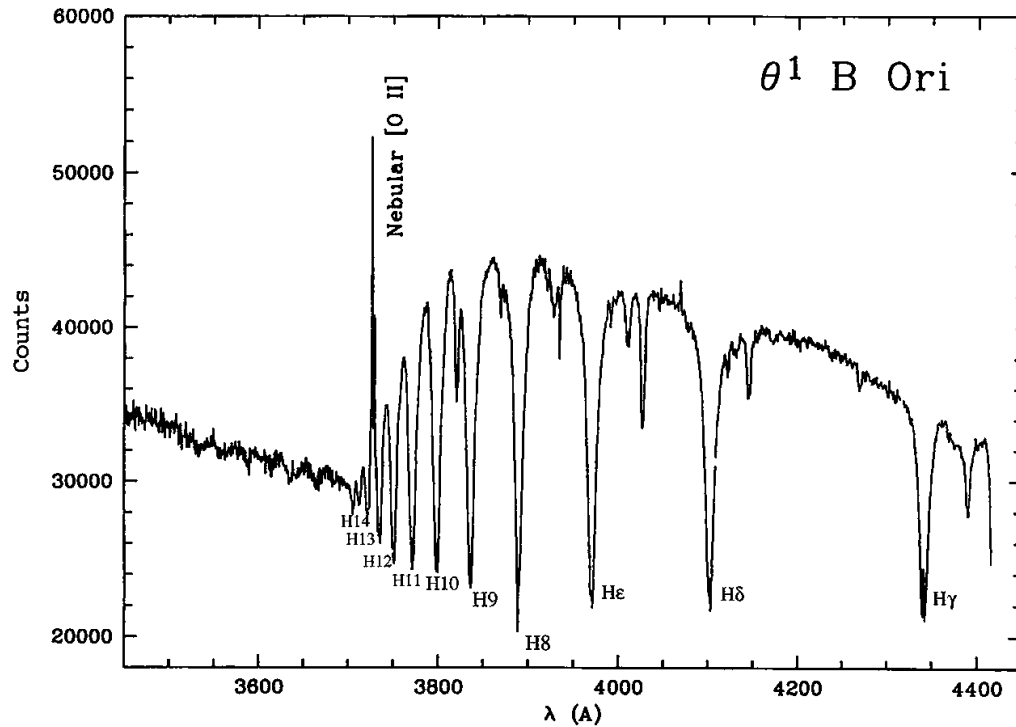


Fig. 3.4 Spectrum of B-type star  $\Theta^1$  B Ori showing Balmer series absorptions recorded at the Anglo-Australian Telescope. (X-W. Liu, private communication.)

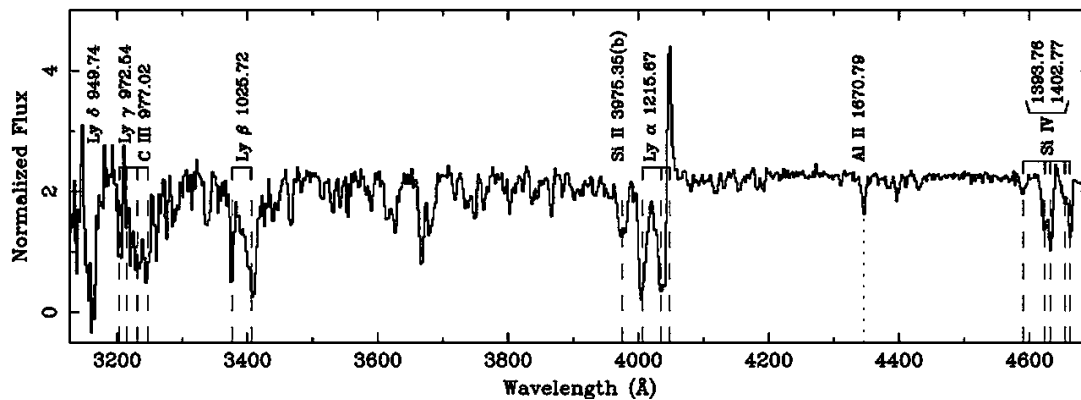


Fig. 3.5 Satellite spectrum recorded from shell nebula GRB 021004. The doublet structure in the Lyman series absorptions is caused by Doppler effects in the shell. [Adapted from N. Mirabel *et al.*, *Astrophys. J.* **595**, 935 (2003).]

D. This particular spectrum was taken as part of a systematic study of the absorption of light from distant quasars which has firmly established the primordial D to H ratio, one of the fundamental parameters of the Big Bang. It should be noted that since deuterium is heavier, its lines should have smaller Doppler widths.

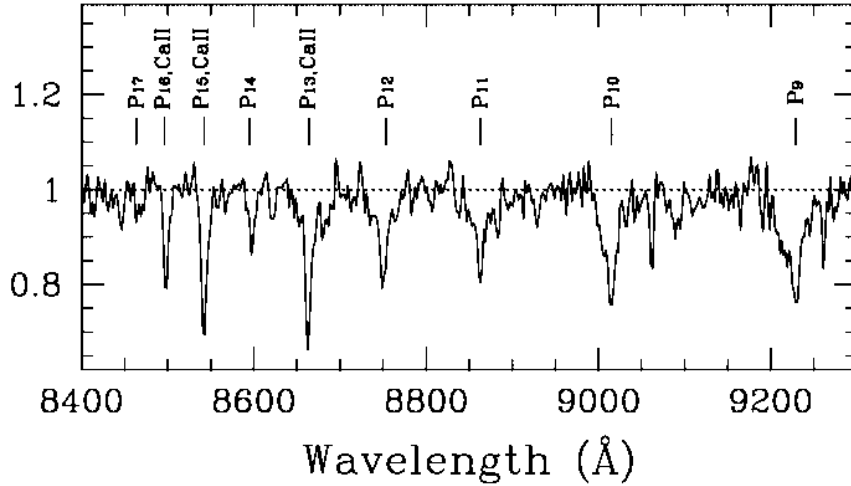


Fig. 3.6 Spectrum soft X-ray transient (SRT) binary star GRO J1655-40 recorded with the Anglo-Australian Telescope, showing higher members of the Paschen series. P13, P15 and P16 are blended with the Ca II triplet transitions discussed in Sec. 6.5. [Adapted from R. Soria, K. Wu and R.W. Hunstedt, *Astrophys. J.* 539, 445 (2000).]

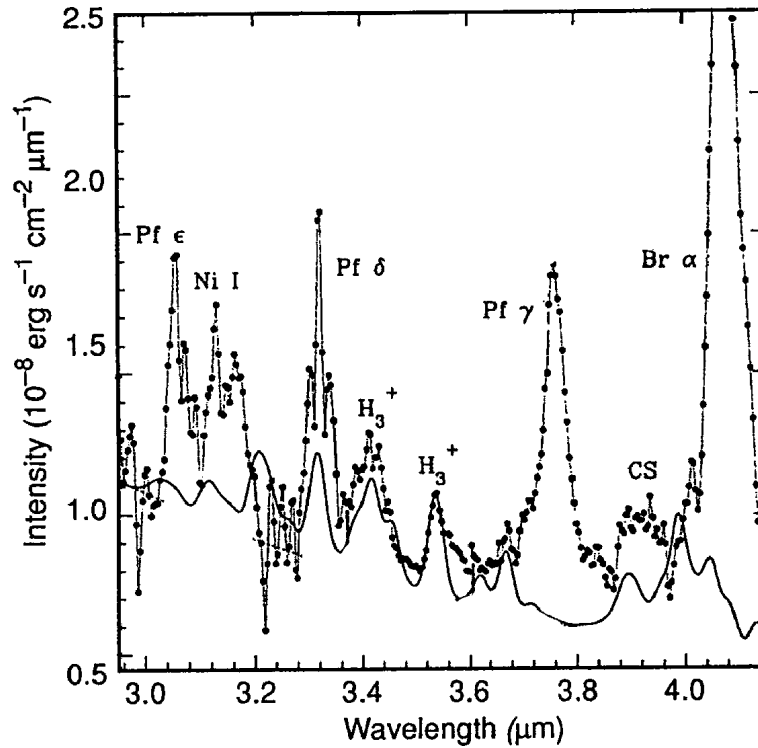


Fig. 3.7 Infrared spectrum of supernova 1987a taken using the Anglo-Australian Telescope 192 days after the initial explosion. Strong Brackett and Pfund emissions from atomic hydrogen are clearly visible. This spectrum gave the first-ever detection of the molecule  $\text{H}_3^+$  outside the solar system; its spectrum is modelled by the solid line. The structure in the spectrum about  $3.2 \mu\text{m}$  is due to telluric effects in this region. [Analysis reported by S. Miller *et al.*, *Nature* 355, 420 (1992).]

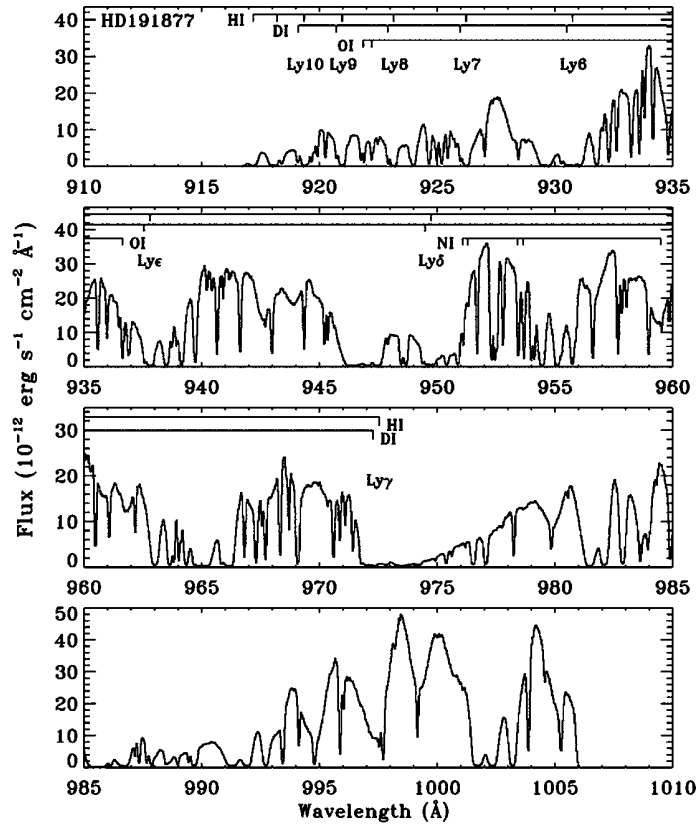


Fig. 3.8 Lyman absorption spectrum for hydrogen and deuterium recorded using the FUSE satellite along a line of sight towards B-type star HD 191877. [Adapted from C.G. Hoopes *et al.*, *Astrophys. J.* **586**, 1094 (2003).]

**Worked Example:** H-atom  $H\alpha$  emission occurs at  $15237 \text{ cm}^{-1}$ . At what wavenumber is the corresponding transition for the D atom?

The Rydberg formula for  $H\alpha$  gives:

$$15237 \text{ cm}^{-1} = R_{\text{H}} \left( \frac{1}{4} - \frac{1}{9} \right). \quad (3.12)$$

The Rydberg constant for deuterium,  $R_{\text{D}}$ , is given by

$$R_{\text{D}} = \frac{\mu_{\text{D}}}{\mu_{\text{H}}} R_{\text{H}}, \quad (3.13)$$

where  $\mu_{\text{H}}$  and  $\mu_{\text{D}}$  are the reduced masses of the hydrogen and deuterium atom, respectively.

$$\frac{\mu_{\text{H}}}{\mu_{\text{D}}} = \frac{M_{\text{H}} + m_e}{M_{\text{H}} m_e} \frac{M_{\text{D}} m_e}{M_{\text{D}} + m_e} = \frac{(M_{\text{H}} + m_e) M_{\text{D}}}{(M_{\text{D}} + m_e) M_{\text{H}}} = 1.00027, \quad (3.14)$$

where the masses  $M_{\text{H}} = 1836.1 m_e$  and  $M_{\text{D}} = 3670.4 m_e$  have been used. Using these numbers gives  $H\alpha$  for D as  $15233 \text{ cm}^{-1}$ , compared to  $15237 \text{ cm}^{-1}$  for H.

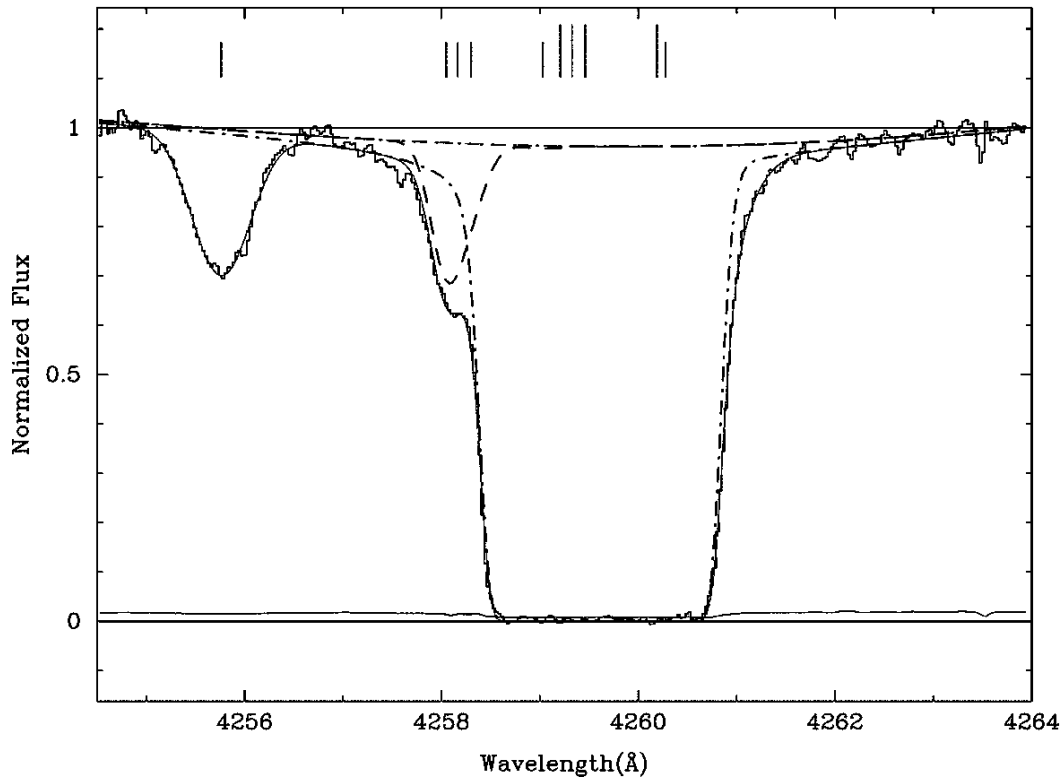


Fig. 3.9 Hubble Space Telescope spectrum of Ly $\alpha$  absorption against quasar QSO 1009+2956 which lies at redshift  $z = 2.5$ . The continuous lines give the results of models which fit several Ly series absorptions. The vertical lines give line centres; the three lines near 4258 Å are due to D; other absorption features are all due to H. [Adapted from S. Burles and D. Tytler, *Astrophys. J.* 507, 732 (1998).]

Although the Rydberg constant is known very precisely, the wavelengths of various transitions in hydrogen do not coincide completely with the values predicted by the Rydberg formula. It should be noted that this formula is only correct within certain assumptions which neglect small effects due to relativity and the finite size of the hydrogen nucleus. For this reason, the measured wavelengths should be used if high accuracy is desired.

### 3.8 H-Atom Spectra in Different Locations

#### 3.8.1 Balmer series

Balmer series lines are the most studied H-atom lines since they are in the visible. Indeed, H $\alpha$  emissions at 6563 Å can be clearly seen with the naked eye as the red light surrounding the Sun during a total eclipse. In fact,

H $\alpha$  and H $\beta$  lines were labelled C and F respectively in Fraunhofer's solar spectrum (see Fig. 1.1).

Stellar envelopes are fairly high density environments. This means that the population of the different atomic energy levels is thermal and given by the Boltzmann distribution:

$$P_i = \frac{g_i}{Q} \exp\left(-\frac{\Delta E_i}{kT}\right), \quad (3.15)$$

where  $P_i$  is the population of the  $i$ th level given as the proportion of the whole population of that atom.  $P_i$  can therefore take values between zero, meaning no atoms in level  $i$ , and one, meaning all the atoms are in level  $i$ . In Eq. (3.15),  $g_i$  is the degeneracy (statistical weight) of level  $i$ , and the energy above the ground state is  $\Delta E_i$ .  $Q$  is the partition function which ensures that the sum over all populations is unity.  $k$  is Boltzmann's constant. When analysing spectra, it is useful to remember that  $k = 0.695 \text{ cm}^{-1} \text{ K}^{-1}$ .

However the temperature,  $T$ , varies between stars, which results in very different spectral characteristics. Since the centre of the star generates bright radiation, spectral lines are seen in absorption. The strength of these absorptions depends on the spectral type of the star.

Hydrogen Balmer lines are strongest for A0 stars which have a temperature of about 10000 K. Few other transitions are seen in these stars. Cooler stars have less population in the  $n = 2$  level of H, so the Balmer line absorption diminishes. Indeed, in the coolest stars ( $T < 5000 \text{ K}$ ), molecules form and little atomic H remains. For stars significantly hotter than 10000 K, H atoms become increasingly ionised and the strength of the Balmer series drops again.

This discussion illustrates a general point. Atoms lose electrons to become ions. As the environment gets hotter, the degree of ionisation increases. Since this is essentially a thermal effect, for every atom, there is a particular ionisation stage which is dominant at a particular temperature. At this temperature, the spectral lines of this ion will be at their strongest. Furthermore, successive ions of particular atoms have spectra quite unlike each other; for example H ions are protons which have no spectrum at all!

Figure 3.10 shows the temperature distribution of iron ions. The Roman numerals in this figure are used to designate ionisation stages. Thus, Fe I corresponds to neutral iron Fe; Fe II to singly ionised iron Fe<sup>+</sup>; Fe III to Fe<sup>2+</sup>, and so forth. Fe XXVI denotes Fe<sup>25+</sup> which is H-like, i.e. it has one electron. Fe XXVII is a bare iron nucleus. Strictly speaking, Roman

numerals label a spectrum, but they are often used to indicate an ion.

For hydrogen, it is usual to talk of H I regions where H is neutral. Often, no optical H-atom spectrum is seen from these regions. Conversely, in H II regions, the H atoms are ionised. As discussed below, H I recombination spectra are seen from H II regions.

Spectra are sensitive to pressure effects. The width of spectral lines depends on pressure, and information on the luminosity class of a star can be obtained by measuring these line-widths. If the pressure is low, higher members of the Balmer series can be seen (see Fig. 3.4). However, the complete series is never observed in stars and the spectrum shows a discontinuity known as the *Balmer jump* (see Fig. 3.11). The jump occurs at the point where continuous (bound-free) absorption switches on. The position of the Balmer discontinuity shifts to longer wavelengths at higher pressure.

To understand why, it is necessary to consider the physical size of the H atom. The approximate radius of the electron orbit in the Bohr atom,  $r_n$ ,

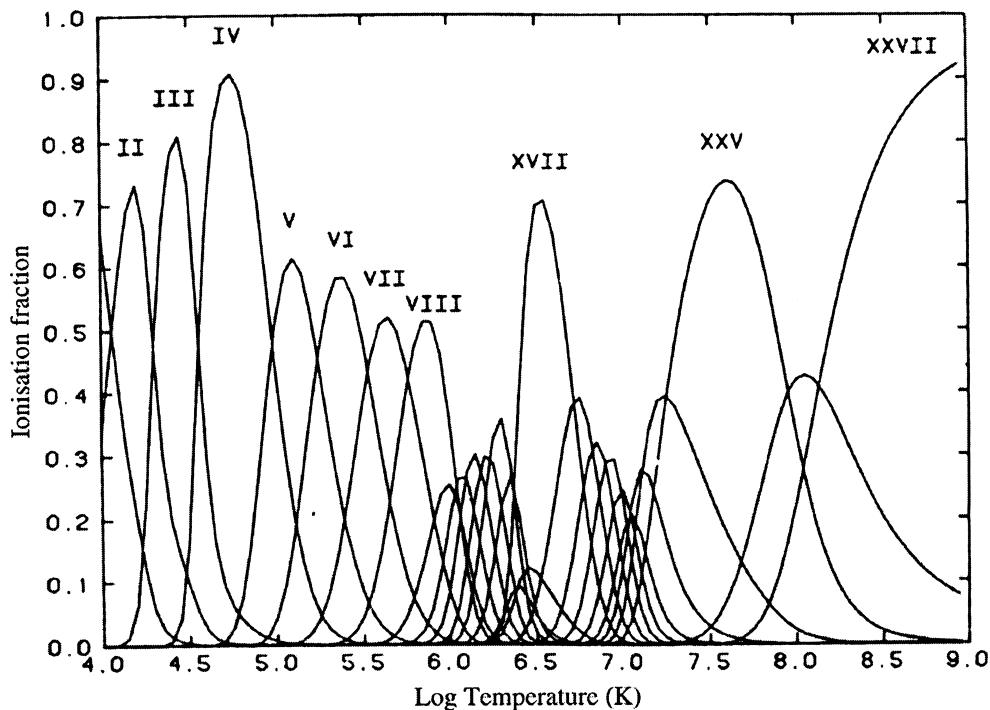


Fig. 3.10 Abundance of iron ions with different ionisation stages as a function of temperature. These results are taken from the coronal model of J.M. Schull. [Adapted from A. Dalgarno and D. Layzer (eds.), *Spectroscopy of Astrophysical Plasmas* (Cambridge University Press, 1987).]

is given by the formula:

$$r_n = n^2 \frac{4\pi\epsilon_0 \hbar^2}{m_e^2 Z} = \frac{n^2}{Z} a_0, \quad (3.16)$$

where for H(1s),  $r_1 = 1 a_0$  and  $a_0 = 0.529 \times 10^{-10}$  m. At high pressure, the mean atom–atom distance will be smaller than some  $r_n$ , and higher orbits will not be found since they will be destroyed by atom–atom collisions.

**Worked Example:** The Sun has a number density,  $N$ , of about  $10^{17}$  cm $^{-3}$ . What is the highest H-atom  $n$  level that one would expect to find? The approximate radius of an electron orbit in the H atom is:

$$r_n = n^2 \times 0.529 \times 10^{-10} \text{ m}.$$

Therefore the approximate volume of an H atom in state  $n$  is

$$V_n \approx \frac{4}{3} \pi r_n^3 \approx \frac{4}{3} \pi n^6 \times 1.48 \times 10^{-31} \text{ m}^3.$$

On the surface of the Sun,  $N \approx 10^{17}$  cm $^{-3} = 10^{23}$  m $^{-3}$ . This means that each atom occupies a maximum volume of about  $10^{-23}$  m $^3$ .

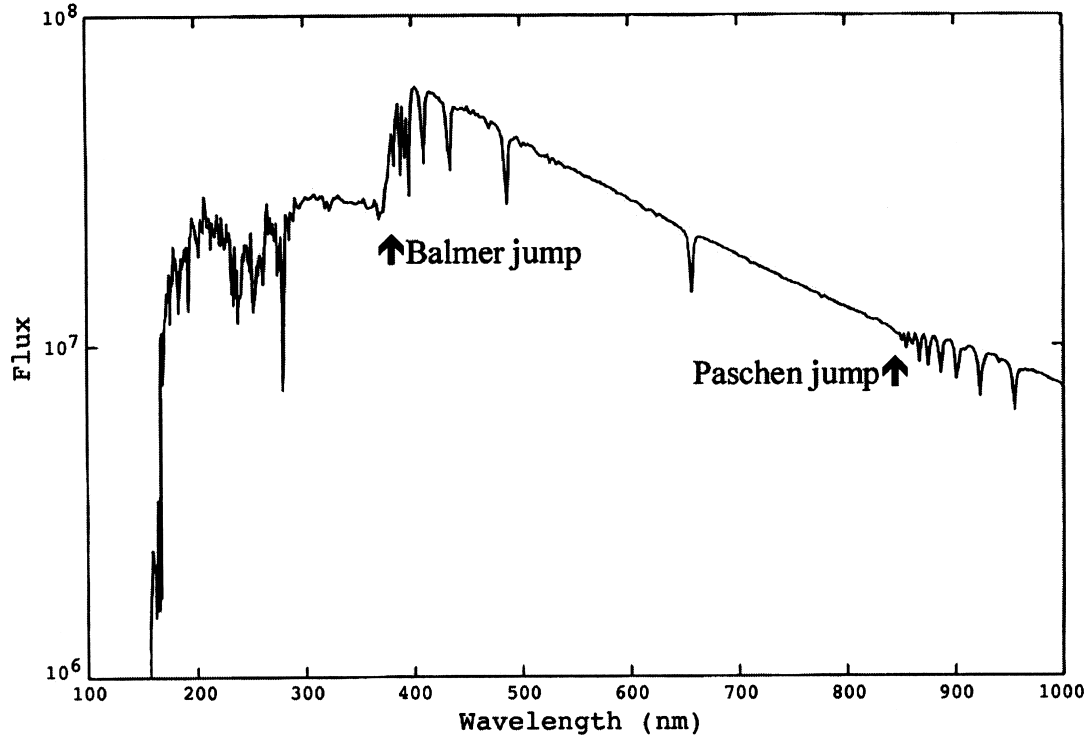


Fig. 3.11 Model spectrum of an A5-type star showing both the Balmer and Paschen discontinuities. (R.J. Sylvester, private communication.)

Assuming that the highest  $n$  value corresponds to the maximum volume allowed for each atom gives

$$\frac{4}{3}\pi n^6 \times 1.48 \times 10^{-31} \approx 10^{-23},$$

which gives  $n \approx 16$  as the highest level that one would expect on the Sun.

### 3.8.2 Lyman series

The Lyman series is expected to be strong in absorption spectra of hot stars which have significant ultraviolet continuum. However, there are a number of technical issues that need to be considered as it is not possible to observe such ultraviolet transitions from the ground.

So far, only a few satellites with the capability of recording spectra this far into the ultraviolet have been launched. The Hubble Space Telescope, for example, does not possess this capability; its best region for spectroscopy is given by  $\lambda \geq 1300 \text{ \AA}$ , whereas  $\text{Ly}\alpha$  lies at  $1216 \text{ \AA}$ . The highly successful International Ultraviolet Explorer (IUE) satellite, which operated for 19 years starting from 1978, covered  $\text{Ly}\alpha$  but no higher Lyman lines. However, this situation changed with the launch of NASA's FUSE (Far Ultraviolet Spectroscopic Explorer) satellite in 1999 (see Fig. 3.8). FUSE covers  $\lambda = 900\text{--}1200 \text{ \AA}$  at good resolution and sensitivity. FUSE's range thus extends below the Ly series limit at  $912 \text{ \AA}$ .

Lyman absorption comes from the H-atom ground state. It is thus dominated by a strong interstellar component. See Fig. 3.9 for an example. Interstellar H atoms are all in their ground states, and are thus only sensitive to Ly wavelengths. This complicates the interpretation of any Ly emission spectrum.

Spectra taken in the locality of the earth are contaminated by strong geocoronal  $\text{Ly}\alpha$  emission (see Fig. 3.12) which is caused by sunlight reflected from H atoms that surround the earth. Such emissions are present in IUE spectra, which were taken in geosynchronous orbit, and also some Hubble Space Telescope spectra, for which Fig. 7.7 gives an example. Figure 10.13, which was recorded with FUSE, shows the clear signature of geocoronal  $\text{Ly}\beta$  emission.

$\text{Ly}\alpha$  can be used as a probe of the Universe at earlier epochs. Quasars emit ultraviolet light with a quasi-continuous distribution. Absorption of this light by H atoms via the  $\text{Ly}\alpha$  transition can be monitored with different epochs being distinguished by their differing redshifts.

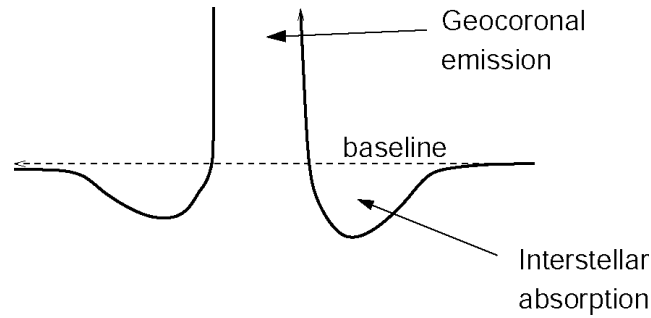


Fig. 3.12 Schematic Lyman  $\alpha$  emission line showing geocoronal emission and, in the wings, absorption against starlight from the interstellar medium.

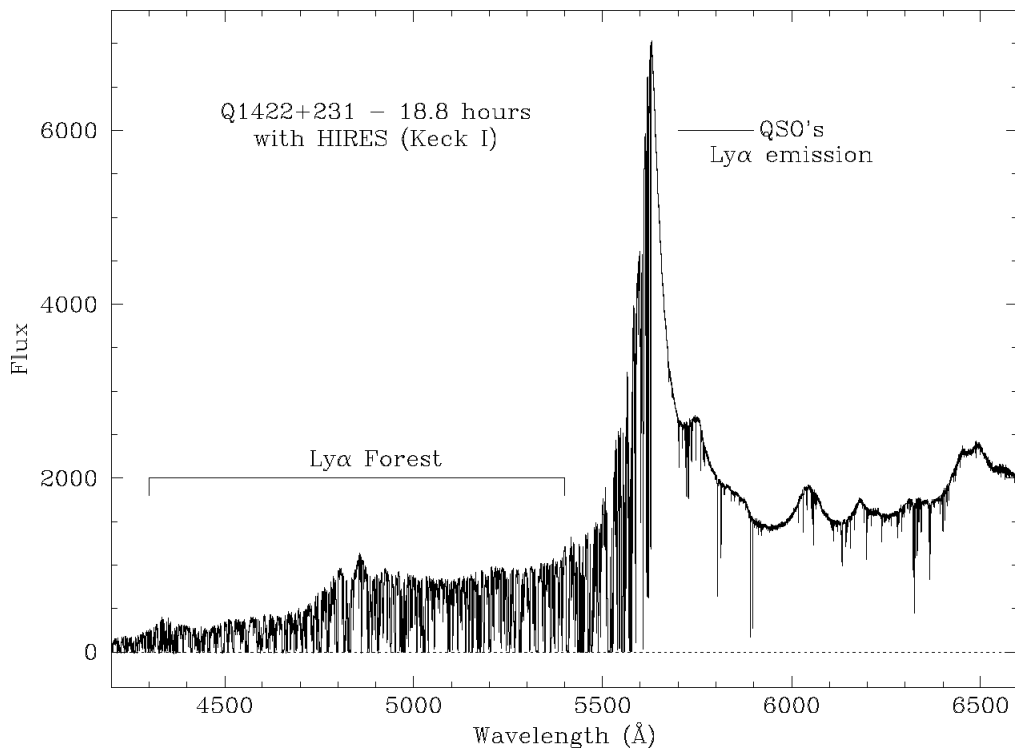


Fig. 3.13 Spectrum of the high redshift QSO Q1422+231, obtained with the High Resolution Echelle Spectrograph on the Keck telescope in Hawaii showing numerous Ly $\alpha$  absorptions by the intervening interstellar medium. These absorptions are known collectively as the *Ly $\alpha$  forest*. (M. Pettini, private communication.)

Figure 3.13 shows a high-resolution spectrum of a high redshift quasar. The strong and broad Lyman  $\alpha$  emission line is observed at a wavelength of  $5622 \text{ \AA}$ , indicating that the quasar is at a redshift  $z = 3.625$ . The spectrum of the quasar at shorter wavelengths is eaten away by a great number of narrow absorption lines. Most of these are single Ly $\alpha$  lines formed in gas located between the quasar and us; they therefore appear at many

discrete redshifts between  $z = 3.625$  and 0. These absorption lines are collectively known as the *Lyman  $\alpha$  forest*. They are a powerful probe of physical conditions in galaxies and the intergalactic medium at early times in the evolution of the universe.

### 3.8.3 Infrared lines

The H-atom series higher than Balmer absorb and emit in the infrared. These can be seen in a number of locations. For example, Fig. 3.7 shows the spectrum of the outer expanding shell of supernova 1987a taken 192 days after the initial supernova explosion. This spectrum was used to report the discovery of the  $\text{H}_3^+$  molecular ion in the expanding gas, however it also shows strong  $\text{Br}\alpha$  emission and several Pfund series lines.

## 3.9 H-Atom Continuum Spectra

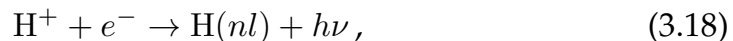
### 3.9.1 Processes

The continuum of a proton and an electron is not quantised. Therefore an H atom in its 1s state can be ionised by any photon with  $\lambda < 912 \text{ \AA}$ , i.e. beyond the Lyman series limit.



This process is called *photoionisation*; it is a bound-free transition. Similarly, the Balmer continuum is observed for  $\lambda < 3646 \text{ \AA}$  (see Fig. 3.11). The probability of photoionisation is greatest when near threshold and drops away as  $\lambda$  decreases. See Fig. 3.14 which illustrates bound-bound and bound-free (photoionisation) spectra for Balmer lines absorbing against the black body radiation curve of a star.

The reverse process,



is called *radiative recombination*; it is a free-bound transition. The probability that an electron will emit a photon as it passes the proton is low, so this is a very unlikely process. However, the chances increase if the electron is travelling slowly, i.e. near threshold.

Radiative recombination is essential, if inefficient, for cooling. For example the recombination era, which started about 300000 years after the Big Bang and lasted for about 1 million years, was the period in which

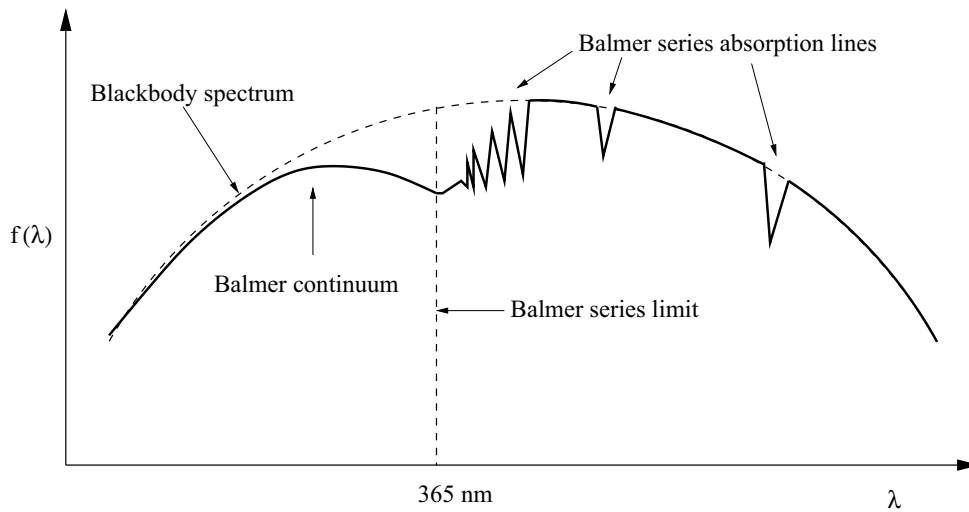


Fig. 3.14 Schematic stellar spectrum showing the hydrogen Balmer lines and continuum. There is a large departure from a black body spectrum at ultraviolet wavelengths below the Balmer series limit.

neutral H and He formed in the early Universe. This is the earliest epoch of our Universe for which it is theoretically possible to record spectra.

### 3.9.2 *H-atom emission in H II regions*

Figure 3.15 shows many higher Balmer lines recorded in Orion. These emissions come from H II regions — ionised regions around hot stars where there are strong ultraviolet fluxes and gases with temperatures of about 10000 K. Under these conditions any H atom will be rapidly photoionised.

Although the recombination of an electron and a proton to produce an H atom is an inefficient process, it still happens continually in H II regions. This produces continuum emissions and a small proportion of neutral H atoms. Typically, about 1% of the protons are in the form of neutral atomic H. Recombination can occur at different levels of the atom. If the atom is formed in an excited level, it can decay by a series of emission lines (see Fig. 3.16). Since the emission lines follow in a series, the process is sometimes referred to as a *cascade*. Different routes are possible and which is preferred depends on the relative values of the different Einstein A coefficients. The ratio of the A coefficients, which determine the relative importance of the competing pathways, are known as *branching ratios*.

H-atom lines from H II regions occur as a result of recombination from the continuum. They are called *recombination lines*.

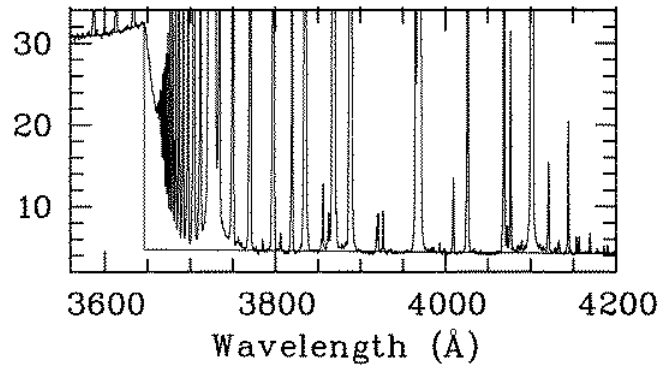


Fig. 3.15 Spectrum of the Orion nebula (M42) recorded using the ESO 1.52 m telescope in Chile. The vertical scale gives the observed flux in units of  $10^{-16} \text{ ergs} \cdot \text{cm}^{-2} \cdot \text{s}^{-1} \cdot \text{Å}^{-1} \cdot \text{arcsec}^{-2}$ . Also shown are polynomial fits to the continuum bluewards and redwards of the Balmer jump at 3646 Å. These can be used to determine the temperature of the nebula. [Adapted from X.-W. Liu *et al.*, *Astrophys. J.* **450**, L59 (1995).]

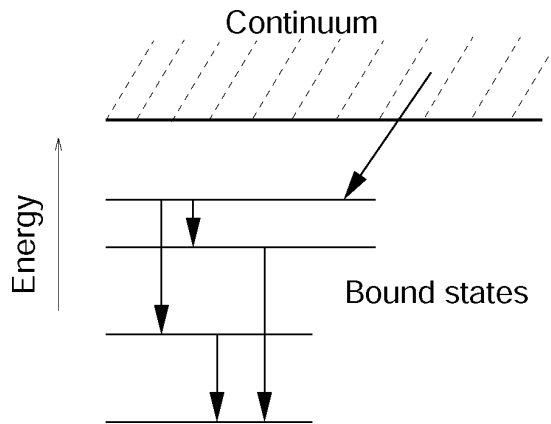


Fig. 3.16 Recombination spectra start with the emission of a continuum photon followed by a cascade of emission lines known as *recombination lines*.

Collisional excitation of H in lower energy levels is not important in H II regions — a ground state atom is much more likely to be photoionised. Populations of different levels are therefore determined by radiative processes and not a Boltzmann distribution.

Recombination and collisional excitation thus form competing mechanisms for driving emission spectra. In H II regions, the most common situation is that while the H-atom spectra are dominated by recombination lines, the spectra of the other atomic species present are driven by collisional excitation. This means that by careful study of both types of emission spectra, one can obtain a measure of both the density and the temperature of the nebula, as well as the strength of the radiation field which drives

Table 3.3 Wavelengths,  $\lambda$ , and Einstein A coefficients for some typical radio frequency hydrogen atom transitions.

	H50 $\alpha$	H50 $\beta$	H50 $\gamma$	H150 $\alpha$
$\lambda$	5.9 mm	3.0 mm	2.1 mm	15.5 cm
$A/s^{-1}$	18	9.4	6.1	0.008

the ionisation process. This means that by studying spectra one can get information on both the nebula and the central star that powers it.

### 3.10 Radio Recombination Lines

As discussed in Sec. 3.8.1, the Balmer series is truncated in the atmospheres of stars by pressure effects. This means that the long wavelength transitions between higher levels cannot be observed. Densities in planetary nebulae are much lower, about  $10^3$ – $10^4 \text{ cm}^{-3}$ , compared to about  $10^{17} \text{ cm}^{-3}$  at the Sun's surface region, or about  $10^{19} \text{ cm}^{-3}$  in the Earth's atmosphere at sea level. At very low densities, bound states with large  $n$  can exist. The Bohr radius for an H atom with  $n = 137$  is approximately  $1 \mu\text{m}$ , meaning that atoms in this state can only survive at densities significantly less than  $10^{12} \text{ particles} \cdot \text{cm}^{-3}$ .

Recombination lines, transitions between neighbouring high values of  $n$ , can be detected at radio wavelengths. These transitions are labelled using a high  $n$  version of the series notation described in Sec. 3.7.

Transitions  $n \leftarrow n + 1$  are called 'H $n\alpha$ ',

Transitions  $n \leftarrow n + 2$  are called 'H $n\beta$ ',

and so forth. It should be noted that 'H' here stands for hydrogen and not Balmer. The transition to state  $n$  is strongest when  $\Delta n = 1$ , i.e. the H $n\alpha$  transition (see Fig. 3.17). Table 3.3 gives wavelengths and lifetimes for some radio-frequency transitions.

Transitions with very high  $n$  have been observed, such as H766 $\alpha$ , where the size of the H atom involved approaches 0.1 mm. Certain lines are observed more than others. For example, the transitions H109 $\alpha$  and H137 $\beta$  both have wavelengths near 6 cm and can be observed at the same time. The H166 $\alpha$  line is near 21 cm, where many detectors are available for observing the so-called *21 cm transition* (see Sec. 3.14).

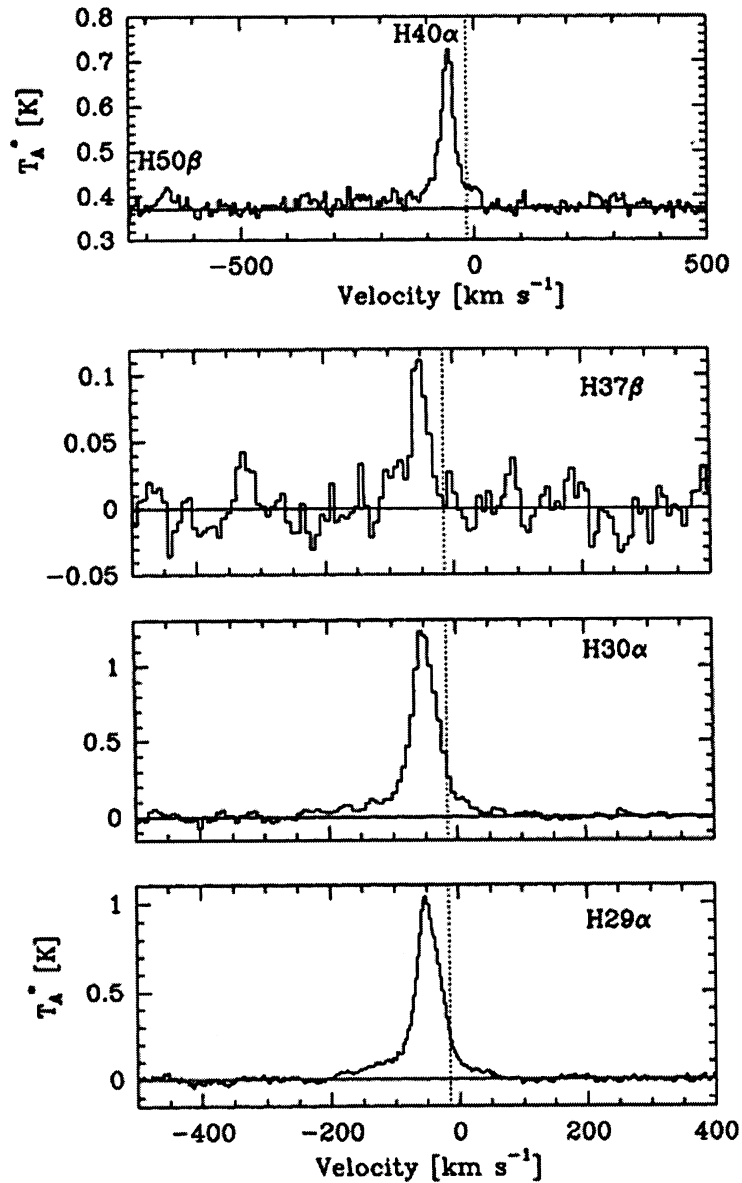


Fig. 3.17 Millimeter wavelength hydrogen radio recombination lines observed toward the very luminous, peculiar star  $\eta$  Carinae using the SEST telescope. Note that the intensity is given by the antennae temperature,  $T_A$ , which is conventional in radio astronomy. [Reproduced from P. Cox *et al.*, *Astron. Astrophys.* **295**, L39 (1995).]

Radio recombination of H atoms can lead to population inversion. Population inversion is one of the conditions necessary for maser (microwave amplified stimulated emission of radiation) action (see Sec. 2.4), a process physically similar to that of a laser. In fact, H atoms can maser in dense H II regions. Such masing has been observed from MCW 349 via the  $n\alpha$  lines. In this location, maser action has been observed for all transitions with  $7 \leq n \leq 90$ . However, molecular masers are much more common

and important than those seen in atomic sources. Molecular masers will be discussed in Sec. 10.5.

### 3.11 Radio Recombination Lines for Other Atoms

An important feature of spectroscopy is that any atom, ion or molecule has a unique spectrum by which it can be readily identified. An exception to this general rule are the radio recombination lines. When a single electron is promoted to a state with a very high principal quantum number,  $n$ , the electron experiences a potential due to the ion core which feels like that due to a single point charge such as a proton. This is because this electron is so far away from the nucleus that the nucleus and the other electrons appear to it as if they occupy a single point.

Under these circumstances the energy levels of the outer electron satisfy the H-atom formula, Eq. (3.8), with an effective nuclear charge,  $Z_{\text{eff}}$ , equal to one. Note that a more sophisticated treatment uses quantum defect theory and replaces  $n^2$  in Eq. (3.8) with  $(n - \mu)^2$ , where  $\mu$  is known as the *quantum defect*. Quantum defect theory is discussed in Sec. 6.1.

Within the confines of the H-atom formula, the only difference between the high  $n$  energy levels, and hence the radio recombination spectrum, of different atoms arises from the different nuclear masses. These different masses give rise to reduced masses, and Rydberg constants, which depend on the atom in question in a fairly simple fashion. The reduced-mass factor differs because the nuclear masses,  $M$ , differ between atoms, giving a scaled Rydberg formula

$$E_n = -\frac{R_\infty}{n^2} \frac{M}{M + m_e}. \quad (3.19)$$

Figure 3.18 gives a sample radio recombination spectrum showing lines from hydrogen, helium and carbon; note that the lines are labelled H, He and C respectively to give the atomic attribution. Radio recombination lines of H and He atoms have been observed from many ionised locations. Lines of heavier atoms such as C have also been detected; indeed radio recombination lines of carbon with  $n$  greater than 1000 have been observed in supernova remnant, Cassiopeia A. Traces of heavier elements, which could be S or Mg, can also be detected sometimes. However as the atoms get heavier, the frequencies of the recombination lines converge (see Table 3.4), making it very difficult to conclusively identify the species involved. Note that in Fig. 3.18 the relative strengths and profiles

Table 3.4 Frequencies,  $f$ , for the  $50\alpha$  radio recombination lines of hydrogen, helium, carbon and an atom with an infinite nuclear mass. The frequencies of the heavier atoms converge on this value.

	H $50\alpha$	He $50\alpha$	C $50\alpha$	$M = \infty$ $50\alpha$
$f/\text{MHz}$	51,072	51,092	51,097	51,099

of He and C lines differ. This is because recombination and hence the emission lines arise from different regions. Helium is only ionised in an inner zone of the H II region which has energetic photons, so it is hot. As a result, the line is strongly Doppler broadened. Conversely, carbon is ionised in cooler regions where even the H is neutral (see Fig. 3.19), so the line is much narrower.

How does the energy balance work in the H II regions from which the recombination emissions are observed? The heating comes from incoming radiation, usually from a central star, which is 'captured' by photoionisation in a bound-free transition:



This is balanced by outgoing radiation, generally at longer wavelengths. This comes in the form of continuum photons formed by recombination,

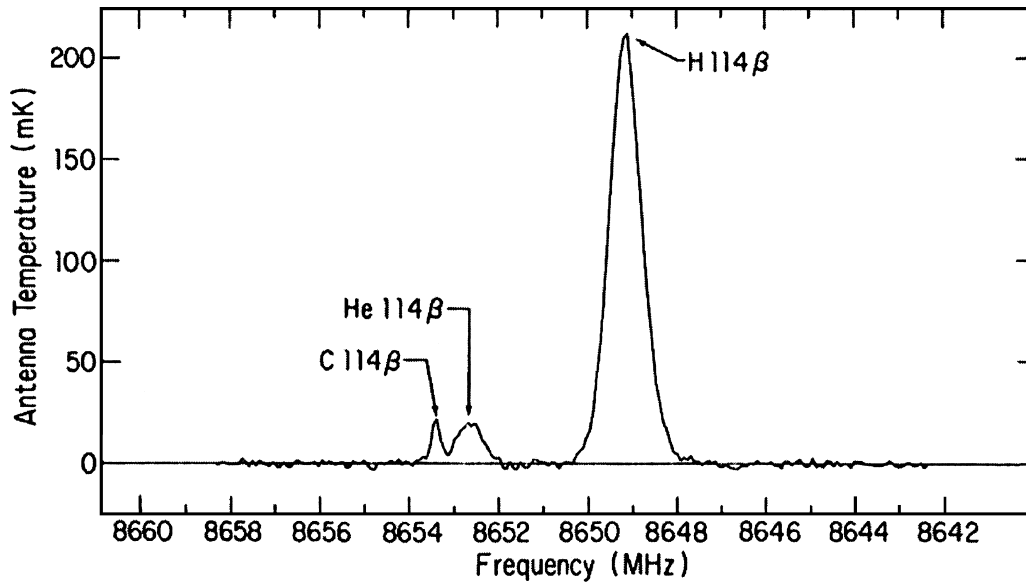


Fig. 3.18 Radio recombination lines of hydrogen, helium and carbon observed in the gaseous nebula W3. [Adapted from A. Dalgarno and D. Layzer (eds.), *Spectroscopy of Astrophysical Plasmas* (Cambridge University Press, 1987).]

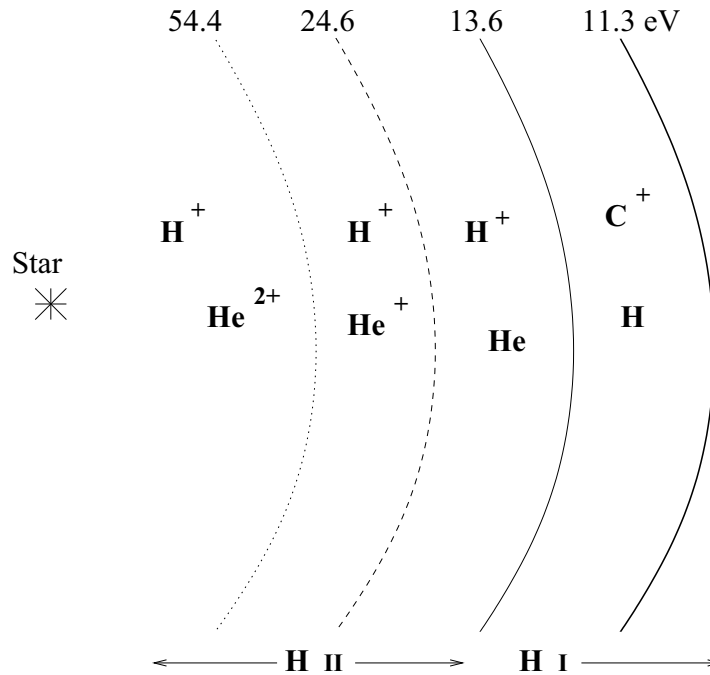


Fig. 3.19 Layers of ionised gas about a central hot star. The figures in eV give the energy required to maintain the ions indicated, and hence the maximum energy of the ultraviolet radiation, found outside each sphere.

the reverse process to Eq. (3.20), and the resulting cascade emissions. It also comes from emissions from heavier atoms and from *bremstrahlung*. *Bremstrahlung*, a German word meaning 'braking radiation', is generated by electrons changing velocities as they pass close to charged nuclei (see Fig. 3.20). *Bremstrahlung* photons are not quantised; they can thus form a continuous distribution in frequency. Such transitions are classified as being free-free transitions as both the upper and lower states are not bound.

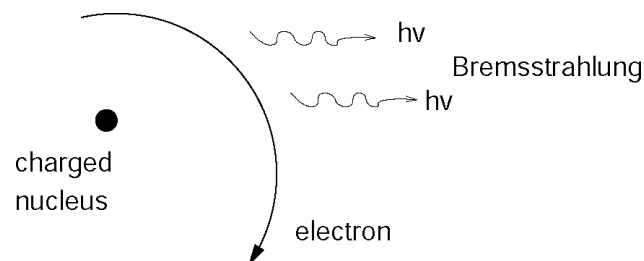


Fig. 3.20 *Bremstrahlung* ('braking radiation') is emitted when a fast electron is slowed down by passing a charged nucleus.

### 3.12 Angular Momentum Coupling in the Hydrogen Atom

One-electron atoms such as hydrogen contain several sources of angular momentum:

- Electron orbital angular momentum  $l$ ;
- Electron spin angular momentum  $s$ ;
- Nuclear spin angular momentum  $i$ .

The nuclear spin arises from the spin coupling of the various nucleons: protons and neutrons both have an intrinsic spin of a half. For atomic spectra it is not necessary to consider the spin of individual nucleons, just their total spin represented by the quantum number  $i$ . For many-electron atoms however, one has to consider the  $l$  and  $s$  quantum number for *each* electron in the system. This situation will be considered in Sec. 4.7.

As in classical mechanics, only the total angular momentum is a conserved quantity. It is therefore necessary to combine angular momenta together. This is best done by adding two angular momenta at a time. The order in which this is done is referred to as a *coupling scheme*. The choice of coupling scheme usually reflects the strength of the actual couplings: the strongest couplings are considered first.

For hydrogen, the usual coupling scheme is to combine  $l$  and  $s$  to give the total electron angular momentum  $j$ . These are added vectorially as

$$\underline{l} + \underline{s} = \underline{j}. \quad (3.21)$$

One then combines the total electron and nuclear spin angular momenta to give the final angular momentum  $f$ :

$$\underline{j} + \underline{i} = \underline{f}. \quad (3.22)$$

To do this one needs to know the rules for addition of angular momenta. This is based on the use of vector addition. Note that angular momentum is a vector as it has both a magnitude and an orientation.

In classical mechanics, adding vector  $\underline{a}$  and vector  $\underline{b}$  gives a vector  $\underline{c}$ , whose length must lie in the range

$$|a - b| \leq c \leq a + b, \quad (3.23)$$

where  $a$ ,  $b$  and  $c$  are the lengths of their respective vectors. This is sometimes known as the *triangulation condition* since the lengths of the vectors must allow the vectors to form a triangle.

In quantum mechanics a similar rule applies except that the results are quantised. The allowed values of the quantised angular momentum,  $c$ , which arise from adding  $a$  and  $b$ , span the range from the sum to the difference of  $a$  and  $b$  in steps of one:

$$c = |a - b|, |a - b| + 1, \dots, a + b - 1, a + b. \quad (3.24)$$

For example, add the two angular momenta  $l_1 = 2$  and  $l_2 = 3$  together to give  $L$ . This is usually written in vector form

$$\underline{L} = \underline{l}_1 + \underline{l}_2, \quad (3.25)$$

and the result is:

$$\begin{aligned} L &= |l_1 - l_2|, |l_1 - l_2| + 1, \dots, l_1 + l_2 - 1, l_1 + l_2, \\ &= 1, 2, 3, 4, 5. \end{aligned}$$

### 3.13 The Fine Structure of Hydrogen

Electron spin arises as part of a relativistic treatment of quantum mechanics. Relativistic effects couple electron orbital angular momentum,  $l$ , and electron spin,  $s$ , to give the so-called fine structure in the energy levels which are split according to the value of the total electron angular momentum  $j$ .

For hydrogen,  $s = \frac{1}{2}$  so that, except for the  $l = 0$  case,  $j = l \pm \frac{1}{2}$  (see Table 3.5). This table labels the resulting levels with the common H-atom notation  $nl_j$ , where  $l$  is given by its letter designations, s, p, d, etc., and by spectroscopic notation for which labels of the  $(^{2S+1})L_J$  are used. A full discussion of spectroscopic notation can be found in Sec. 4.8.

Table 3.5 shows the fine structure levels of the H atom. This table shows that the states with principal quantum number  $n = 2$  give rise to three fine-structure levels. In spectroscopic notation, these levels are  $2^2S_{\frac{1}{2}}$ ,  $2^2P_{\frac{1}{2}}^o$  and  $2^2P_{\frac{3}{2}}^o$ .

So far the discussion on H-atom levels has assumed that all those with the same principal quantum number,  $n$ , have the same energy. In other words, the energy does not depend on  $l$  or  $j$ . This is not correct: inclusion of relativistic (or magnetic) effects split these levels according to the total angular momentum quantum number  $j$ . This splitting, called *fine structure*, has been well-studied in the laboratory. An even more subtle effect called the *Lamb shift*, which is due to quantum electrodynamics, can also be observed. Values of these splittings for the  $n = 2$  levels are given in Fig. 3.21.

Table 3.5 Fine structure effects in the hydrogen atom: splitting of the  $nl$  orbitals due to fine structure effect for  $l = 0, 1, 2, 3$ . The resulting levels are labelled using H atom notation, and the more general spectroscopic notation of terms and levels (see Sec. 4.8).

Configuration	$l$	$s$	$j$	H atom	Term	Level
$ns$	0	$\frac{1}{2}$	$\frac{1}{2}$	$ns_{\frac{1}{2}}$	$n^2S$	$n^2S_{\frac{1}{2}}$
$np$	1	$\frac{1}{2}$	$\frac{1}{2}, \frac{3}{2}$	$np_{\frac{1}{2}}, np_{\frac{3}{2}}$	$n^2P^o$	$n^2P^o_{\frac{1}{2}}, n^2P^o_{\frac{3}{2}}$
$nd$	2	$\frac{1}{2}$	$\frac{3}{2}, \frac{5}{2}$	$nd_{\frac{3}{2}}, nd_{\frac{5}{2}}$	$n^2D$	$n^2D_{\frac{3}{2}}, n^2D_{\frac{5}{2}}$
$nf$	3	$\frac{1}{2}$	$\frac{5}{2}, \frac{7}{2}$	$nf_{\frac{5}{2}}, nf_{\frac{7}{2}}$	$n^2F^o$	$n^2F^o_{\frac{5}{2}}, n^2F^o_{\frac{7}{2}}$

For hydrogen, fine-structure and Lamb-shift splittings are too small to be important for most astronomical applications. The fine structure is, however, of great importance for complex atoms and will be discussed further in Chapters 4 and 6.

### 3.14 Hyperfine Structure in the H Atom

There is one more source of angular momentum in the H atom which has not yet been included. This is the nuclear spin,  $i$ ; for H,  $i = \frac{1}{2}$ . Coupling  $i$  to the total electron angular momentum,  $j$ , gives the final angular momentum,  $f$  [see Eq. (3.22)]. For H this means

$$f = j \pm \frac{1}{2}. \quad (3.26)$$

The ground state of H is  $1s_{\frac{1}{2}}$  or  $^2S_{\frac{1}{2}}$  and has  $j = \frac{1}{2}$ . This means that nuclear spin coupling can split this state into two levels with  $f = 0$  or  $1$ . There is a very small,  $6 \times 10^{-5}$  eV, splitting between the lower  $f = 0$  and higher  $f = 1$  levels of H caused by magnetic effects. The  $f = 0-1$  transition between these levels has a frequency of 1420.406 MHz which

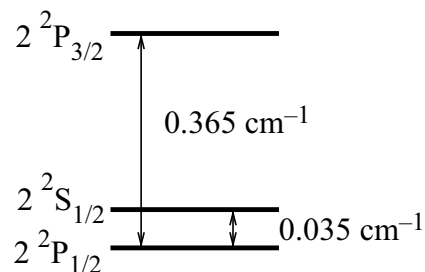


Fig. 3.21 Splitting in the  $n = 2$  levels of atomic hydrogen. The larger splitting is the fine structure and the smaller one the Lamb shift.

corresponds to a wavelength of 21 cm. The 21 cm line is probably the single most important line in astronomy. It is used to map H-atom densities throughout the ISM (see Fig. 3.22 for example).

The 21 cm line is a powerful tool because:

- (1) Displacement of the line gives the line-of-sight velocity;
- (2) Its intensity gives the number of atoms. Note that the line is very weak, its Einstein A coefficient is  $2.9 \times 10^{-15} \text{ s}^{-1}$  which corresponds to a lifetime of 10 million years, so it is always optically thin;
- (3) The line profile can be used to deduce the temperature of the gas. Thus, for example, Fig. 3.22 suggests that location G23.437-0.207 is much cooler than G43.172+0.006, where the lines appear to be significantly Doppler broadened.
- (4) The Zeeman splitting of the transition can be used to measure the magnetic fields, see Chapter 8.

Note that the line is seen in both emission and absorption and its analysis can be complicated by the presence of several clouds along any particular line of sight.

### 3.15 Allowed Transitions

For hydrogen, transitions which correspond to any change in the principal quantum number,  $\Delta n$ , are allowed. However transitions are not observed between all states of the H atom or indeed complex atoms. Transitions are

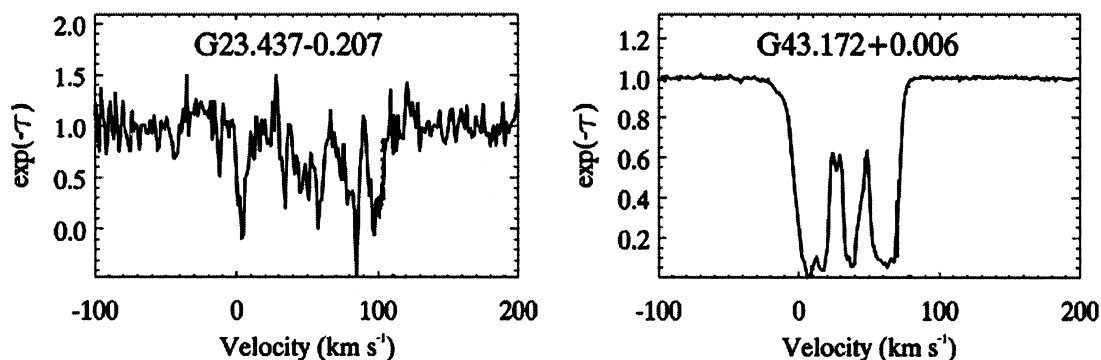


Fig. 3.22 21-cm-line profiles observed with the Very Large Array for two galactic lines of sight recorded as part of a study which constructed a face-on galactic map of the H II region complexes. The vertical axis of the spectra represents the observed line-to-continuum intensity, which is equivalent to  $\exp(-\tau_{\text{line}})$ . [Adapted from M.A. Kolpak *et al.*, *Astrophys. J.* **582**, 756 (2003).]

governed by selection rules which determine whether they can occur. The selection rules can be derived rigorously using the rules of quantum mechanics [see Schiff (1969) in further reading], but will simply be stated here.

Strong transitions are driven by electric dipoles. Weaker transitions, driven by both electric quadrupoles and magnetic dipoles, are observed astronomically (see Sec. 5.2), but are not important for hydrogen. Rigorous quantum mechanical analysis shows that for electric dipole transitions in hydrogen:

$$\begin{aligned}\Delta n & \text{ any;} \\ \Delta l & = \pm 1; \\ \Delta s & = 0, \text{ (for H this is always satisfied as } s = \frac{1}{2} \text{ for all states);} \\ \Delta j & = 0, \pm 1; \\ \Delta m_j & = 0, \pm 1.\end{aligned}$$

The last selection rule on  $m_j$  is only important in a magnetic field.

Thus if one considers the  $H\alpha$  transition which corresponds to  $n = 2-3$ , the  $\Delta l = \pm 1$  condition shows that not all transitions between sub-levels occur. Specifically, the transitions  $2s-3p$ ,  $2p-3s$  and  $2p-3d$  are allowed whereas the transitions  $2s-3s$ ,  $2p-3p$  and  $2s-3d$  are not allowed.

If fine structure effects are considered, then the selection rules can give further constraints. Considering only the  $H\alpha$  transitions designated allowed above, the selection rule on  $j$  shows that

$$\begin{aligned}2s_{\frac{1}{2}} - 3p_{\frac{1}{2}} & \text{ is allowed;} \\ & - 3p_{\frac{3}{2}} \text{ is allowed;} \\ 2p_{\frac{1}{2}} - 3d_{\frac{5}{2}} & \text{ is not allowed;} \\ & - 3s_{\frac{1}{2}} \text{ is allowed;} \\ & - 3d_{\frac{3}{2}} \text{ is allowed;} \\ 2p_{\frac{3}{2}} - 3s_{\frac{1}{2}} & \text{ is allowed;} \\ & - 3d_{\frac{3}{2}} \text{ is allowed;} \\ & - 3d_{\frac{5}{2}} \text{ is allowed.}\end{aligned}$$

### 3.16 Hydrogen in Nebulae

Hydrogen atom emissions in H II regions and planetary nebulae are very similar but the latter are generally brighter, which means that more weak line emissions can be observed. In particular, lines belonging to the Balmer

Table 3.6 Lifetimes,  $\tau$ , for decay by spontaneous emission for low-lying excited states of the hydrogen atom.

Level	2s	2p	3s	3p	3d
$\tau/s$	0.14	$1.6 \times 10^{-9}$	$1.6 \times 10^{-7}$	$5.4 \times 10^{-9}$	$2.3 \times 10^{-7}$

series are often seen strongly in emission. Indeed, the characteristic red colour seen in many nebulae comes from  $H\alpha$ .

Balmer or other spectral series are obtained from excited atoms spontaneously emitting photons. Every excited state has a half-life  $\tau$ , similar to that encountered in radioactive decay, which is related to the strength of emission. Thus excited states which decay only by weak line emission are long-lived and those which decay via strong transitions are short-lived. However, most excited states can emit to more than one other state.

The lifetime of excited state  $i$  is given by

$$\tau_i = \left( \sum_j A_{ij} \right)^{-1}, \quad (3.27)$$

where  $A_{ij}$  is the Einstein A coefficient (see Sec. 2.2).

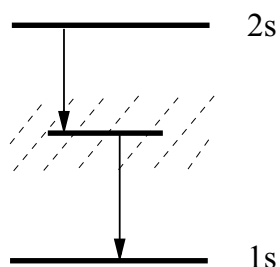


Fig. 3.23 Decay of the metastable 2s state of hydrogen giving two continuum photons.

Lifetimes for allowed atomic transitions are short, perhaps a few times  $10^{-9}$  s. Table 3.6 gives some examples for the H atom. A glaring exception in Table 3.6 is the lifetime of the 2s level of H. This state has a lifetime of  $\sim 0.14$  s, i.e. it lives  $10^8$  times longer than the 2p state. This is because the transition  $2s \rightarrow 1s$  is strongly forbidden. The 2s state is metastable which means that on the atomic scale, it is long-lived.

So how does the 2s state decay? By the process of two-photon emission, which is an inefficient process and in this case has an Einstein A coefficient of  $7 \text{ s}^{-1}$  which can be compared to  $A(2p \rightarrow 1s) = 6.3 \times 10^8 \text{ s}^{-1}$ .

The combined energy of the photons emitted must correspond to the energy difference  $E(2s) - E(1s)$  but the photons themselves can take any energy within this constraint (see Fig. 3.23). The photons thus appear as continuous emission radiation. Indeed the two-photon decay of the H 2s state is responsible for approximately one half the continuum emission observed from H II regions.

## Problems

- 3.1 Give an expression for the energy levels of the hydrogen atom in terms of the Rydberg constant  $R_H$ . Assuming a value  $R_H = 109677.58 \text{ cm}^{-1}$ , derive a wavenumber for the Ly $\alpha$  transition of atomic hydrogen in  $\text{cm}^{-1}$ . Explain why the Rydberg constant,  $R_\infty = 109737.31 \text{ cm}^{-1}$ , is more appropriate than  $R_H$  for a heavy one-electron atom. Hence obtain an estimate for the wavenumber of the Ly $\alpha$  transition of hydrogen-like iron,  $\text{Fe}^{25+}$ . From what astronomical environments would such transitions occur and how might they be observed?
- 3.2 A proton and an electron recombine to form atomic hydrogen in its 4p state. At what wavelengths will recombination lines be observed? Label each wavelength by its standard series notation. How would the observed emissions differ if the atoms had recombined to the 4s level?
- 3.3 Hydrogen H $\alpha$  has a rest wavelength of 6564.71 Å. At what rest wavelength would you expect to observe deuterium H $\alpha$ ? What telescope resolution ( $R = \frac{\lambda}{\Delta\lambda}$ ) would be required to resolve this difference? How does this compare to the resolution required to resolve H and D Ly $\alpha$  transitions? Given a high enough resolution telescope, what other problems do you anticipate in obtaining the  $\frac{D}{H}$  abundance by observing a single spectral line such as H $\alpha$ ? The mass of H is 1836.1 and D is 3670.4 in atomic units. In these units the mass of an electron is one.
- 3.4 A typical star has a number density,  $N$ , of about  $10^{16} \text{ cm}^{-3}$ , while in an H II region the number density is more typically  $10^4 \text{ cm}^{-3}$ . In each case what is the highest level of atomic hydrogen that is likely to be occupied? State any assumptions made in obtaining this answer. The partition function for atomic hydrogen can be written as:

$$z = \sum_{n=1}^{\infty} 2n^2 \exp\left(-\frac{R_H}{n^2 kT}\right).$$

This series cannot be summed as it diverges. Can you suggest why, in practical astronomical applications, the partition function for the H atom is finite?

- 3.5 Use the Rydberg formula to obtain the wavelength of the  $80\alpha$  radio line for an atom of infinite mass. Hence, taking the mass of the hydrogen nucleus to be 1836.1 electron masses, obtain the frequency of the  $80\alpha$  transition of atomic hydrogen. What resolving power would be required to separate the two transitions?